



HAL
open science

Effect of molecular weight on crystallization behavior of poly (lactic acid) under isotherm and non-isotherm conditions

Nader Zirak, Mohammadali Shirinbayan, Sedigheh Farzaneh, Abbas Tcharkhtchi

► **To cite this version:**

Nader Zirak, Mohammadali Shirinbayan, Sedigheh Farzaneh, Abbas Tcharkhtchi. Effect of molecular weight on crystallization behavior of poly (lactic acid) under isotherm and non-isotherm conditions. *Polymers for Advanced Technologies*, 2022, 33 (4), pp.1307-1316. 10.1002/pat.5603 . hal-03637088

HAL Id: hal-03637088



<https://hal.science/hal-03637088>

Submitted on 11 Apr 2022

HAL is a multi-disciplinary open access archive for the deposit and dissemination of scientific research documents, whether they are published or not. The documents may come from teaching and research institutions in France or abroad, or from public or private research centers.

L'archive ouverte pluridisciplinaire **HAL**, est destinée au dépôt et à la diffusion de documents scientifiques de niveau recherche, publiés ou non, émanant des établissements d'enseignement et de recherche français ou étrangers, des laboratoires publics ou privés.

Effect of molecular weight on crystallization behavior of poly(lactic acid) under isotherm and non-isotherm conditions

Nader Zirak¹  | Mohammadali Shirinbayan¹  | Sedigheh Farzaneh²  |
Abbas Tcharkhtchi¹ 

¹Arts et Metiers Institute of Technology, CNRS, CNAM, PIMM, HESAM University, Paris, France

²P4Tech, 23 Rue du 8 Mai 1945, Boissy Saint Leger, France

Correspondence

Nader Zirak, Arts et Metiers Institute of Technology, CNRS, CNAM, PIMM, HESAM University F-75013 Paris, France.
Email: nader.zirak@ensam.eu

Abstract

The effect of molecular weight on the crystallization behavior of poly(lactic acid) (PLA) both isothermally and non-isothermally was studied using differential scanning calorimetry and polarized optical microscopy. Two distinct crystal forms (α and α') were investigated under normal conditions of crystallization for different molecular weights. Using microscopy, the growth rate of spherulites was measured and the nucleation rate was estimated. Heterogeneous nucleation and morphology with a variant α and α' forms have been proposed. Spherulites from low molecular mass PLA contained more interlamellar amorphous phase. In addition, the results showed more rapid crystallization of α' than the α form in isothermal conditions.

KEYWORDS

crystallization, kinetic, PLA, polymorphism, spherulites

1 | INTRODUCTION

Poly(lactic Acid) (PLA) is a biodegradable polyester produced from natural sources.^{1–3} Due to its biocompatibility, bioresorbability,⁴ transparency, and suitable mechanical properties, PLA has various applications in medical, packaging, and automobile industries.^{1,5}

Crystallization is a mainly thermodynamic phenomenon that can be characterized as the passage from a disordered structure in the rubbery state to a more ordered (crystalline) structure in the glassy state and is accompanied by a release of heat called “latent heat”.^{4,6} The key important role of crystallization on flexural modulus, strength,⁷ and enzymatic degradation⁸ of PLA has been studied in the literature.

Like many semi-crystalline polymers, PLA is polymorphic. In general, different crystallization conditions can lead to formation of four α , α' (or δ), β , γ crystalline forms.⁹ Zhang et al.¹⁰ have shown that the formation of the α form will take place at temperatures above 120°C, while the α' form is formed at temperatures below 100°C. In other words, the α' form undergoes a solid–solid transformation during heating to the α form. The α form undergoes an improvement during heating by melting–recrystallization, as it can be observed on other non-polymorphic polymers.

The crystallization of polymers, whether in isothermal or non-isothermal conditions, can be described by the Kolmogorov,¹¹ Avrami,¹² and Evans¹³ models. These models, by considering the fraction of volume which transformed into the crystalline volume as a function of time or temperature, can provide the α transformation rate information. Considering the key role of crystallization in optimization of processing conditions and the properties of the end products, analysis of crystallization kinetics in isothermal¹⁴ and nonisothermal¹⁵ conditions and calculation of activation energy of crystallization^{16,17} have been studied extensively. Several factors affect the kinetics of crystallization of PLA: molecular mass,^{18,19} content of enantiomers of the lactic acid group,^{19,20} types of crystals,²¹ chemical modifications,^{22,23} nucleating agent^{24,25} and even type of terminations of the macromolecular chains.²⁶ Pan et al.²¹ have studied the effect of molecular weight of poly(L-lactide) (PLLA) on polymorphous crystallization and melting behavior. They showed that by increasing the M_w the crystallization rate drops greatly. Yong et al.²⁷ have investigated kinetics of PLLA crystallization in isothermal conditions. According to their results, heterogeneous nucleation followed by 3-dimensional growth was observed, also by decreasing the M_w the crystal growth rate increased.

PLA is characterized by slow crystallization kinetics, that is, low nucleation rates and slow spherulitic growth compared to the other

semi-crystalline polymers.^{14,28} Under isothermal conditions, the crystallization of PLA, depending on molecular weight, can be observed in the range of $70^{\circ}\text{C} < T_c < 150^{\circ}\text{C}$.²⁹ In non-isothermal conditions, crystallization seems to disappear for cooling rates greater than $10^{\circ}\text{C}/\text{min}$.^{30,31} Half-crystallization times with crystallization temperature (T_c) in isothermal experiments show a discontinuity between 110 and 120°C consistent with spherulitic growth rate measurements in isothermal or non-isothermal conditions over the same temperature range.²⁹ This transition can disturb the Gaussian crystallization and affect the crystallization kinetics. This transition by disturbing the Gaussian crystallization can affect the crystallization kinetics. In the study by Zhang et al.¹⁰ considering the presence of α' form for $T_c < 120^{\circ}\text{C}$, discontinuity is attributed to the polymorphism of PLA and the variation of the kinetic parameters of this new form.

Several authors have attempted to demonstrate the polymorphism of PLA. This polymorphism results in the appearance of two distinct crystal forms (α and α') under normal conditions of crystallization. According to these works, the form α develops at high temperature and the form α' at low temperature, while for intermediate temperatures, the two crystalline forms can coexist. Structure-property relationships and thermodynamic,^{32,33} mechanical properties,³⁴ or even barrier properties³⁴⁻³⁶ of the α and α' forms have been studied.

In this contribution, given the necessity of considering the existence of each crystalline form to establish a model with a precise description of its crystallization kinetics, investigation of crystallization in isothermal and non-isothermal conditions play a key role. Regarding, this paper deal with the crystallization behavior from the melt of PLA in two conditions of isothermal and non-isothermal. The detailed characterization of the crystalline phase of PLA with respect to the growth rate of spherulites and the crystallization half time for the different molecular weights was studied.

2 | MATERIALS AND EXPERIMENTAL PROCEDURE

2.1 | Material

PLA under the grad of Natureworks Ingeo Serie 3000 (PLA NW 30) was purchased from ICO Polymers company. Its average molecular weight (M_w) was 101,000. PLA was dried for 10 h at 80°C before processing.

2.2 | Sample preparation

For sample preparation and achieving different molecular weights, hydrolysis method was used as a degradation method. PLA has the advantage of being highly hydrolyzable due to its biodegradable nature. The hydrolytic degradation of PLA is characterized by a mechanism of random chain cleavages, making it possible to split the

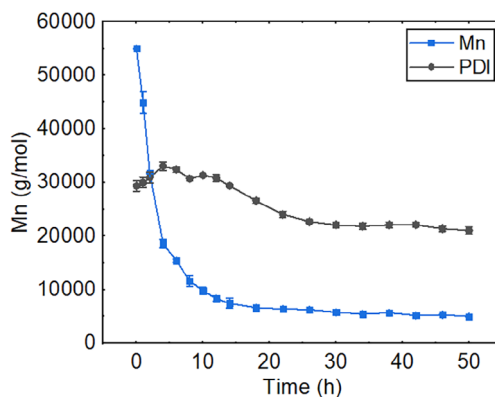


FIGURE 1 Mn and polydispersity index results of poly lactic acid hydrolysis from chromatography analysis. Error bars are standard deviation

macromolecular chain, without excessively influencing the distribution characterized by the polydispersity index (PI).

The hydrolysis of PLA was performed with distilled water at neutral pH, at a temperature of 100°C for 1, 2, 4, 6, and 14 h. In a reflux assembly containing a 5 L flask, 40 g of PLA was added to 4 L of water. During each experiment, 2 g of PLA was extracted from the medium. In addition, the fresh distilled water was exchanged with each sample to maintain the neutrality of the environment. Then the samples were dried in an oven at 80°C . The molecular weight was measured by chromatographic analysis. Figure 1 shows the number average molecular mass (Mn) and polydispersity index (PDI) against the hydrolysis time. As can be seen, Mn was varied between approximately 55,000 and 5000 g/mol over the 50 h of hydrolysis. Sample codes, as well as specific information on the various samples, are reported in Table 1.

2.3 | Thermal analysis

Thermal properties of PLA were investigated using differential scanning calorimetry (DSC—TA Instruments Q1000) under a nitrogen sweep to avoid any oxidation of the material. Each test was carried out using 10 mg of sample powder inserted into a sealed non-hermetic aluminum capsule. The samples are then treated by the protocols presented in Table 2.

2.4 | Polarized optical microscopy

An optical microscope (Olympus BH2-UMA) with a digital camera, an analyzer, and a crossed polarizer were used as well as a first-order delay plate in red ($\lambda = 530$ nm) coupled to a Linkam CSS450 heating plate. The CSS450 plate is equipped with a water-cooling system, ensuring precise control of the temperature ($\pm 0.2^{\circ}\text{C}$) and the cooling rate (from 0.01 to $30^{\circ}\text{C}/\text{min}$). Pressing and controlling the thickness of samples between 1 and 2500 μm were achieved using a motor.

TABLE 1 Sample codes, time of hydrolysis, and molecular mass data

The time of hydrolysis (h)	Mn (g/mol)	M_w/M_n	Sample code
0	55,000	1.9	Mn 55000
1	45,000	2.1	Mn 45000
2	32,000	2.1	Mn 32000
4	19,000	2.2	Mn 19000
6	10,000	2.2	Mn 10000
14	7500	2	Mn 7500

TABLE 2 Differential scanning calorimetry analysis protocols

Isothermal protocol	Non-isothermal protocol
Ramp with 30°C/min up to 200°C	Ramp with 30°C/min up to 200°C
5 min isotherm at 200°C	5 min isotherm at 200°C
Ramp with 30°C/min up to T_{c_iso}	Ramp with cooling speed φ_r up to 25°C
Isothermal for a duration T_{c_iso}	Ramp with heating speed φ_c up to 200°C
Ramp with 30°C/min up to 25°C	

The samples with 2 μm thickness were made at 200°C. Before cooling, to allow relaxation of samples, they were kept at 200°C for 5 min. The images were recorded when the crystallization temperature was reached for the isothermal tests and from the start of cooling for the non-isothermal condition. Depending on the crystallization condition the time between each photograph was between 1 and 120 s. Image processing was carried out using ImageJ software.

3 | RESULTS AND DISCUSSION

3.1 | Effect of molecular weight

3.1.1 | Isothermal crystallization profiles: transformation rate and enthalpy analysis

Considering the important effect of molecular weight on crystallization,^{37,38} effect of different molecular weights on crystallization of PLA were investigated. Isothermal crystallization of the samples was analyzed through the isothermal thermograms. Crystallization was analyzed in the temperature range of 85–145°C. Figure 2 shows the relative crystallinity against the time for Mn 55000. According to this figure, results show a sigmoidal dependence with time. Half-time of crystallization ($t_{1/2}$) can be determined from this results, this time was in the range of 6–200 min depending on selected temperature.

Figure 3 shows the enthalpy of crystallization against temperature. According to this figure, enthalpy of crystallization was increased

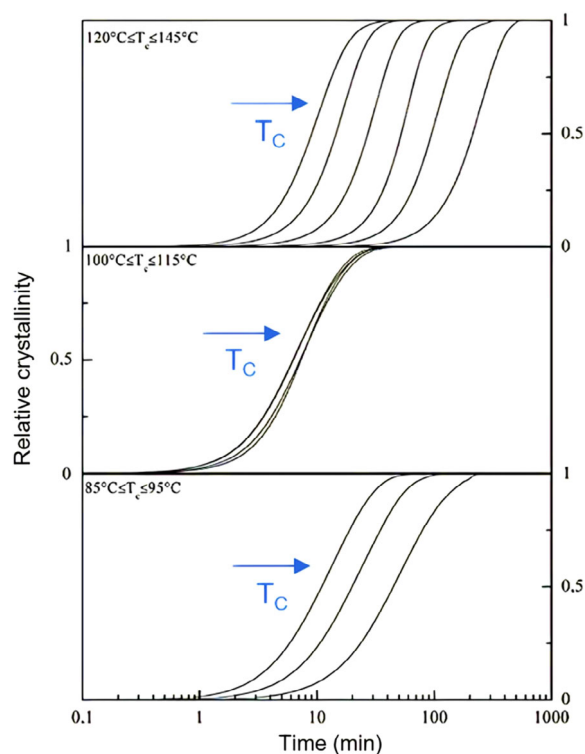


FIGURE 2 Evolution of relative crystallinity versus the crystallization time at various temperatures for Mn 55000

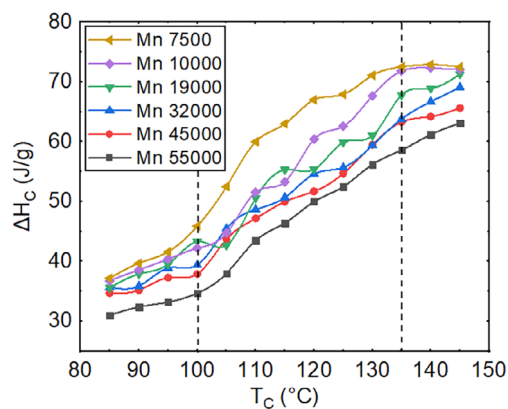


FIGURE 3 Isothermal enthalpy of crystallization

by increasing the temperature. Also, samples with lower molecular mass showed higher enthalpy. This phenomenon is in good agreement with the fact that the crystals formed at higher temperatures would have a greater thickness and stability, indicating that a greater amount of energy was released during their formation.³⁹ On the other hand, lower molecular weight can cause better macromolecules mobility resulting in lower defects formation within the crystallites. Therefore, the higher stability of crystals with short chain molecules results in releasing a greater amount of energy during their formation.

The intense increase in the enthalpy of crystallization can also be attributed to the existence of the two crystalline forms having been attributed to the thermodynamic properties (ΔH_f°).^{32,33} Also,

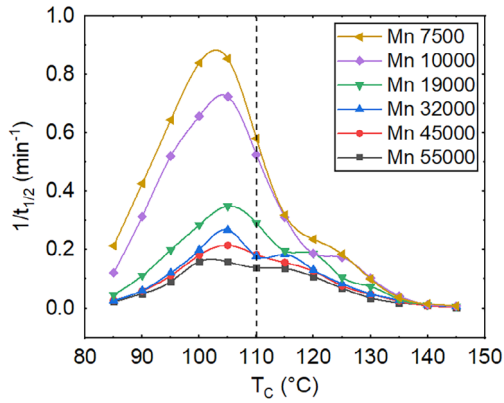


FIGURE 4 Growth rate as a function of crystallization temperature for different molecular weights

according to Figure 3, the slope change is evident for all samples at crystallization temperatures of 100 and 135°C, which transition can be attributed to α and α' . Obviously, α' is the disordered form and is less stable compared to the α . Consequently, it appears logical that the crystallinity rate of α' is lower so the transition will be different.

For characterization of crystallization kinetics, the time necessary to reach 50% of crystallization, that is, half-crystallization time ($t_{1/2}$), at each temperature for the samples was calculated. Figure 4 shows $t_{1/2}$ as a function of temperature for all samples; the fastest was observed at 105°C. It should be noted that a transition exists between 110 and 115°C, which is independent of molecular mass, and that it characterizes a variation of the crystallization mechanism in this temperature interval. Di Lorenzo,⁴⁰ Yasuniwa et al.,⁴¹ and Pan et al.²¹ have also reported this behavior.

3.1.2 | Non-isothermal crystallization: transformation rate and enthalpy analysis

In this section, crystallization of the polymer with different molecular weights with respect to the non-isothermal condition was analyzed. The thermal response for cooling rates between 0.5 and 20°C/min was measured. Figure 5 shows the crystallization thermograms for the series of considered speeds. According to this figure, peak of crystallization temperature was decreased by increasing the cooling rate. It can be noted that the PLA NW30 exhibits no crystallization maxima when the cooling rate was greater than 10°C/min.

Non-isothermal thermograms analysis showed recrystallization or cold crystallization for many cooling rates. The observation of cold crystallization during the second heating is characteristic of an incomplete crystallization during cooling. According to the results, the crystallization maxima was decreased by increasing the cooling rate.

Considering the definition of relative transformation rate which is referred to the volume occupancy rate per the crystalline entities or the primary crystallization rate, the process reaches the end when the is equal to 1. It can also contain a part of secondary crystallization corresponding to the thickening of the crystalline lamellae at the end

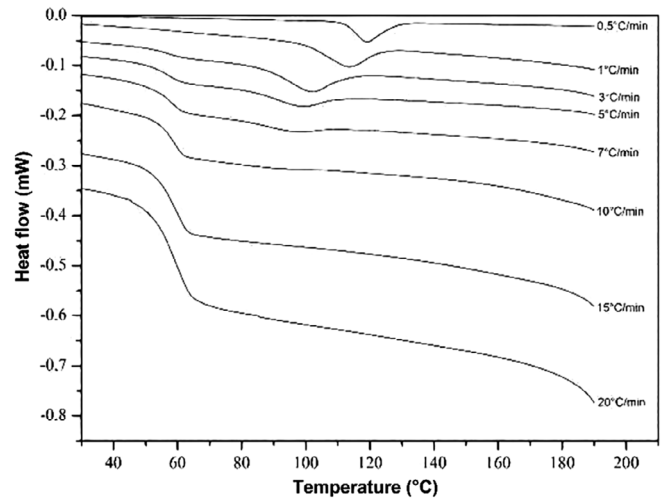


FIGURE 5 Thermogram of crystallization of the initial poly lactic acid between 0.5 and 20°C/min

of the transformation. In this case, the transformation was not completed during cooling, and completing it occurred during the second heating. The sum of the enthalpies of crystallization and recrystallization is considered the total enthalpy of crystallization. A non-isothermal cooling can be considered as a succession of isothermal cooling. The non-isothermal enthalpy of crystallization approximately represents the weighted average of transformation rates at a given temperature, over the temperature interval where the cooling takes place for the isothermal enthalpy. Therefore, in each case, peak crystallization temperature (T_p), enthalpy of crystallization (ΔH_c) and enthalpy of recrystallization (ΔH_{cc}) were calculated (Table 3). Note that $\Delta H_c + \Delta H_{cc}$ is relatively consistent for different cooling rates. However, they tend to decrease with the rate of cooling, where deviations for low molecular masses were up to 10 J/g.

For more analysis, the T_p value which is in the temperature range of two crystalline forms coexists (95°C < T_p < 120°C) was investigated. The quantities of each form of α and α' can be various depending on the cooling rate. Differences in thermodynamic properties of α and α' forms have been suggested by Rathi et al.³² and Kalish et al.³³ by measuring their equilibrium enthalpies. So, different quantities of α or α' forms in the samples will lead to the different enthalpy of crystallization.

One can note that the change of the maxima in crystallization and the observed enthalpy fluctuations can be due to the quantities of α and α' forms. The quantity of the α and α' forms in a crystallized sample under iso-thermal and non-isothermal conditions can be quantified by Equation (1):

$$X_T = 1 - \frac{1}{1 + \exp\left(\frac{T_c - T_{1/2}}{v}\right)}, \quad (1)$$

where x is the quantity of α form, T_c shows the crystallization temperature, and v represents the transformation rate. Consequently, by

TABLE 3 Enthalpy values and real transformation rate for different molecular weight

Mn 55000										Mn 32000									
φ (°C/m)	T_p (°C)	ΔH_c (J/g)	ΔH_{cc} (J/g)	$\Delta H_c + \Delta H_{cc}$ (J/g)	α_{reel} final	T_p (°C)	ΔH_c (J/g)	ΔH_{cc} (J/g)	$\Delta H_c + \Delta H_{cc}$ (J/g)	α_{reel} final	T_p (°C)	ΔH_c (J/g)	ΔH_{cc} (J/g)	$\Delta H_c + \Delta H_{cc}$ (J/g)	α_{reel} final				
0.5 ± 0.01	119.3	48.3	0	48.3	1	119.4	49.2	0	49.2	1	119.9	51.7	0	51.7	1				
1 ± 0.01	113.4	41.5	4.8	46.3	0.90	113.7	51	0	51.0	1	114.4	53	0	53.0	1				
2 ± 0.01	104.3	29.2	14.6	43.8	0.67	105.8	41	11.0	52.0	0.79	106.7	48.7	7.3	56.0	0.9				
3 ± 0.01	101.7	16.9	23.8	40.7	0.42	102.6	28	21.5	49.5	0.57	104.2	32.5	20.9	53.4	0.6				
4 ± 0.01	99.7	9.2	31.9	41.1	0.22	100.6	15.7	34.4	50.0	0.31	102.0	24.8	27.9	52.7	0.5				
5 ± 0.01	98.5	5.6	35.7	41.3	0.14	98.9	13.1	37.6	50.7	0.26	100.7	15.5	36.4	51.9	0.3				
6 ± 0.01	97.3	4.1	38.4	42.5	0.10	98	7.5	42.2	49.7	0.15	99.1	9.9	41.9	51.8	0.2				
7 ± 0.01	96.4	2.8	40.7	43.5	0.06	97	5.5	43.1	48.7	0.11	98.3	7.4	46	53.4	0.1				
8 ± 0.01	96.6	2.2	41.4	43.6	0.05	96.1	3.3	47.2	50.5	0.07	96.8	5.2	48.8	53.6	0.1				
9 ± 0.01	95.3	1.4	42.2	43.6	0.03	95.1	2.3	48.3	50.6	0.05	95.8	4.4	47.1	51.5	0.1				
10 ± 0.01	94.1	0.7	44.8	45.5	0.01	94.8	1.9	47.3	49.2	0.04	95.1	2.3	49.7	52.0	0.1				
Mn 19000										Mn 7500									
φ (°C/m)	T_p (°C)	ΔH_c (J/g)	ΔH_{cc} (J/g)	$\Delta H_c + \Delta H_{cc}$ (J/g)	α_{reel} final	T_p (°C)	ΔH_c (J/g)	ΔH_{cc} (J/g)	$\Delta H_c + \Delta H_{cc}$ (J/g)	α_{reel} final	T_p (°C)	ΔH_c (J/g)	ΔH_{cc} (J/g)	$\Delta H_c + \Delta H_{cc}$ (J/g)	α_{reel} final				
0.5 ± 0.01	122.5	56.5	0	56.5	1	124.7	62.3	0	62.3	1	123.4	63.5	0	63.5	1				
1 ± 0.01	117	58.4	0	58.4	1	121.6	66.6	0	66.6	1	121.3	67.3	0	67.3	1				
2 ± 0.01	108.1	52.3	0	52.3	1	109.9	60.5	0	60.5	1	115.8	62.2	0	62.2	1				
3 ± 0.01	105.5	42.4	11.9	54.3	0.78	108.2	56.6	0	56.6	1	107	59	0	59	1				
4 ± 0.01	103.6	35	17.4	52.4	0.67	105.3	53.5	0	53.5	1	105.1	55	0	55	1				
5 ± 0.01	101.6	31.6	21.6	53.2	0.59	103.4	48.9	10	58.9	0.83	103.3	53.3	3.1	56.4	1				
6 ± 0.01	100.5	23.8	29.6	53.4	0.45	102.9	47.7	10.7	58.4	0.82	102	51	5.1	56.1	0.9				
7 ± 0.01	99.3	16	35.6	53.5	0.31	101.3	38	17.8	55.8	0.68	100.7	47.5	10.8	58.3	0.8				
8 ± 0.01	97.9	13.3	38.1	51.4	0.26	101.1	34	21.7	55.7	0.61	99.1	43.3	9.8	53.1	0.8				
9 ± 0.01	97.2	9.2	42.1	51.3	0.18	99.1	32.2	20.9	53.1	0.61	95.6	40	12.9	52.9	0.8				
10 ± 0.01	96.6	6.2	46.2	52.4	0.12	97.6	21.4	32	53.4	0.40	96.9	34.5	20.1	54.6	0.6				

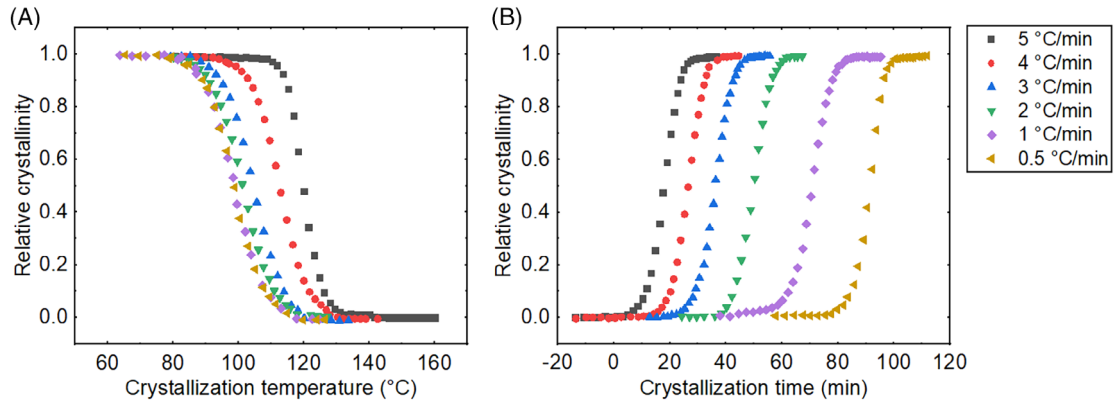


FIGURE 6 (A) Relative crystallinity versus crystallization temperature and (B) relative crystallinity versus crystallization time at different cooling rates for Mn 55000

considering a transformation rate of 1 at the end of the second heating, $\Delta H_c + \Delta H_{cc}$ represents the total enthalpy of crystallization. The rate of real transformation at the end of cooling (noted $\alpha_{\text{real final}}$) for each cooling rate was calculated according to Equation (2):

$$\alpha_{\text{real final}} = \frac{\Delta H_c}{\Delta H_c + \Delta H_{cc}} \quad (2)$$

The times of corresponding crystallizations were calculated according to Equation (3):

$$t = \frac{T_{\text{max}} - T}{\varphi} \quad (3)$$

With $T_{\text{max}} = 160^\circ\text{C}$ and φ the cooling rate. The actual transformation rates can easily be deduced by Equation (4).

$$\alpha_{\text{real}(T)} = \alpha_{\text{real final}} \times \alpha(T) \quad (4)$$

Figure 6 represents the curve of relative crystallinity versus crystallization temperature and crystallization time with respect to the different cooling rates. According to the figure, the half-time of crystallization ($t_{1/2}$) was determined for each condition. The sigmoidal shape can be observed from all the achieved shapes. The results show three different stages in crystallinity, so that, primary 0–0.2 relative crystallinity is related to the induction period and the relative crystallinity of more than 0.8 can be attributed to the occurrence of a secondary crystallization process causing to slower crystallization and completing of crystals in the latter stages.⁴²

Figure 7 shows the enthalpy of crystallization against the cooling rate. According to the results, all the samples, except Mn 55000, show a plateau value for $1^\circ\text{C}/\text{min}$. The appearance of a plateau value suggests that crystallization was completed on the cooling rate. However, this is not the case for all the samples based on the calculated real transformation rates. Indeed, from Mn 19000 even if the maximum transformation rate has been reached, the measured crystallization enthalpy continuously increased by decreasing the cooling rate.

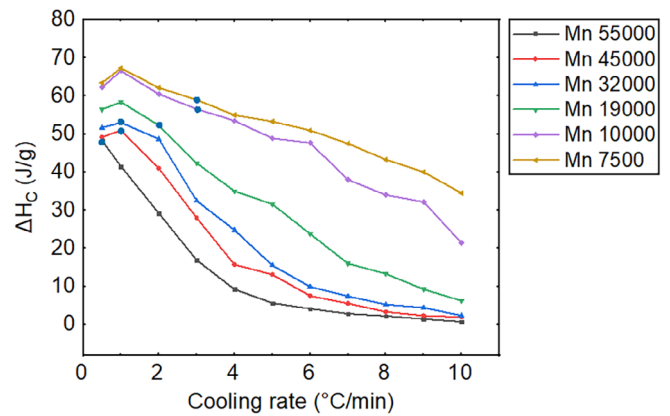


FIGURE 7 Crystallization enthalpy as a function of the cooling rate for different molecular mass

In addition, the markers corresponding to the rates for transformation degree of 1 is obtained are added in Figure 8. This behavior is most certainly linked to the rate of α and α' forms contained in the crystalline phase formed. Indeed, for each molecular mass, the crystallization zone is almost the same considering the T_p values. It can be said that the rate of α and α' forms in each sample for a given cooling rate is substantially the same. In fact, it is necessary to consider the crystallization kinetics of the α and α' forms and the influence of the molecular mass on these kinetics. Obtained results for $t_{1/2}$ in isothermal condition showed a more quick crystallization of α' form compares to the α form. Moreover, the crystallization kinetics for each of the forms was increased by decreasing the molecular mass.

3.2 | Microscopic analysis

The microscopic analysis was performed in isothermal condition at the temperature range of $85\text{--}145^\circ\text{C}$ for each sample. Morphology of the crystal structure was investigated by analyzing the micro-kinetic parameters such as growth rate (G) and nucleation rate (N) necessary for the kinetic analysis.

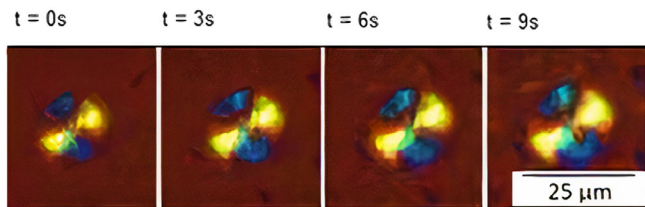


FIGURE 8 Growth of a spherulite for Mn 7500 at 125°C

3.2.1 | Crystal growth

The growth rate over the isothermal temperature has been measured. For each temperature, at least five spherulites have been considered. In the case of weak nucleations, the experiments have been repeated to obtain five measurements.

The measurement is relatively simple for high crystallization temperatures, since the crystal entities are sufficiently large. In this regard, the measurement method, which proposed and verified by Di Lorenzo⁴⁰ was used. This method consists of the formation of a few spherulites at a high temperature in an isothermal condition during cooling. Once these spherulites are sufficiently grown and clearly observable, the sample was cooled rapidly to the crystallization temperature of the test. The growth of the previously created spherulites is then followed. The growth of the spherulites is illustrated in Figure 8, which represents the Mn 7500 at 125°C for the time interval of 3 s between each image.

A linear evolution of the radius of the spherulites was observed over time. The slope of these lines that is related to the growth rate was obtained by linear regression. Therefore, for each T_C , the growth rate of the five spherulites was considered, then the standard deviation has been calculated (measurement error of $\pm 0.05 \mu\text{m}/\text{min}$). The evolution of the G as a function of T_C is plotted in Figure 9. One can note that the evolution of growth rate is marked by a discontinuity between 110 and 115°C, which is in agreement with the literature.⁴³ So, this behavior in the growth of the α and α' forms can be concluded to the difference in kinetics. Given that a maximum G was around 130°C confirms the α form has a faster growth rate compared to the α' form. This observation contrasts in the literature for the PLLA, where the maximum is observed between 105 and 110°C. This phenomenon is linked to the quantity of motif D present in the PLA NW30. Tsuji et al.²⁰ showed that the contribution of the α' form to the growth rate decreases by the quantity of D form is varied in a sample of PDLA. In addition, the measured semi-crystallization times show that the α' form has kinetics much faster than the α form. It can be concluded that the kinetics of crystallization of PLA is strongly influenced by nucleation.

3.2.2 | Estimation of nucleation

Due to the high nucleation densities observed from 115°C, estimation of nucleation was performed from 120°C. Indeed, most spherulites were similar diameters, which suggest that they were formed at the

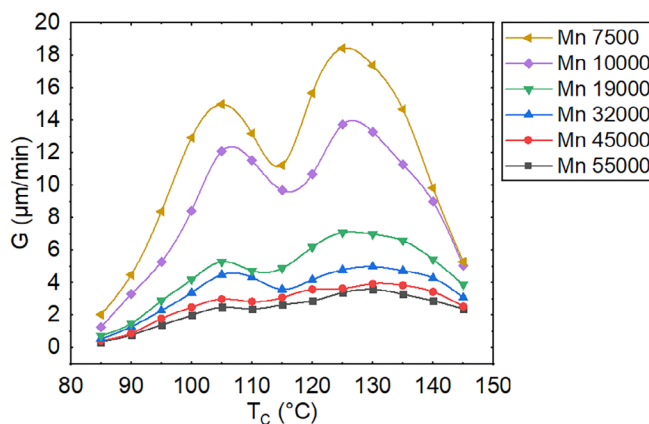


FIGURE 9 Growth rate measurement by polarized optical microscopy

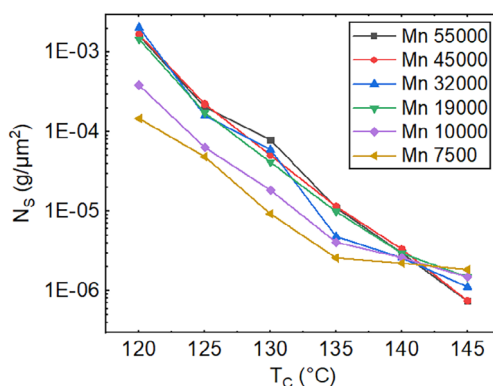


FIGURE 10 Estimation of the nucleation rate by polarized optical microscopy

same time. However, the presence of smaller spherulites suggesting a sporadic small portion of nucleation. Generally, nucleation was heterogeneous during transformation. The nucleation rate was measured by estimating the number of spherulites developed at each crystallization temperature. In addition, when the nucleation rate became too high, in order to increase the uncertainty, counting was performed over a smaller area.

Figure 10 shows the rates of nucleation per unit area on a logarithmic scale as a function of crystallization temperature. The plot shows a linear evolution from 130°C for all the samples. For the highest temperatures, a low number of spherulites was observed on the analyzed surface. According to the results, it can be said that for the Mn 55000 to Mn 19000 the nucleation rates are almost similar in comparison with the Mn 10000 and Mn 7500 which have lower nucleation density.

3.2.3 | Crystal morphology

Two samples of Mn 55000 and Mn 10000 for the analysis of crystal morphology were chosen at different temperatures. Figure 11 and Figure 12 present the formation of spherulites for Mn 55000 and Mn

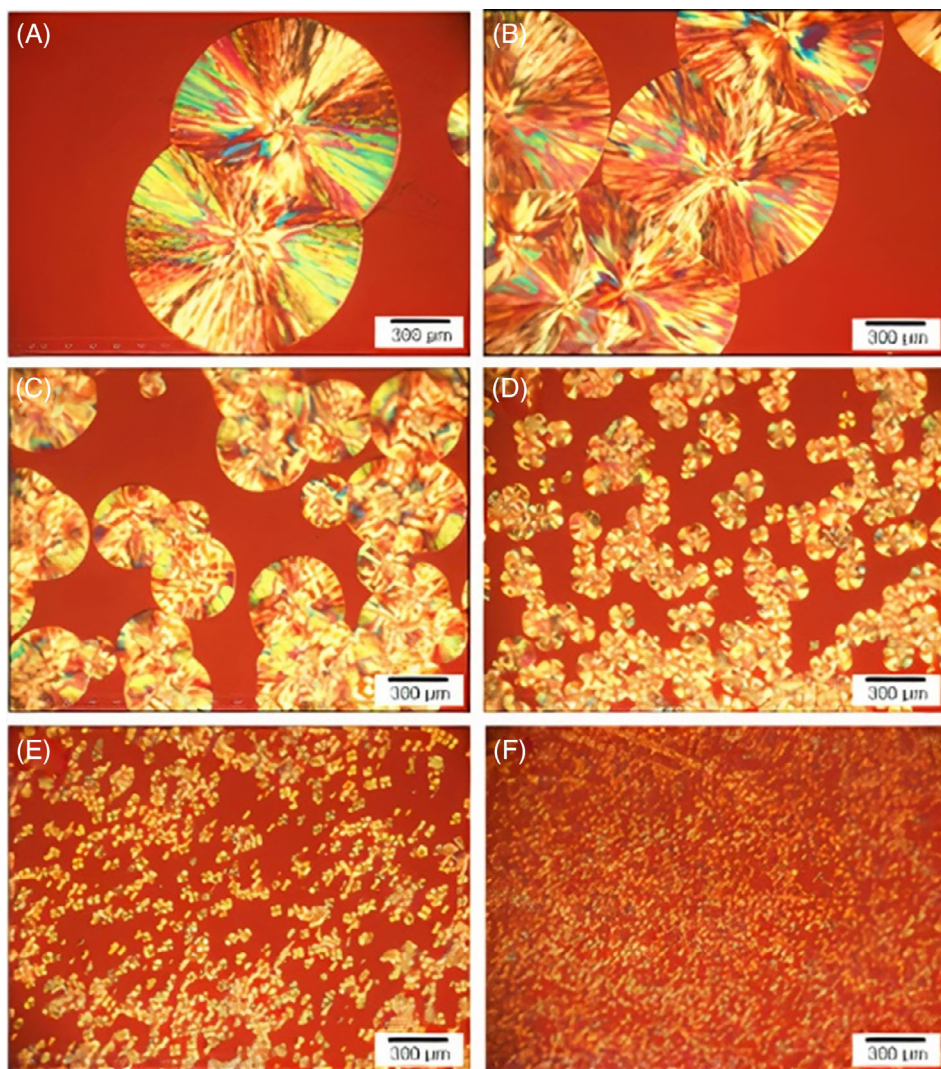


FIGURE 11 Crystallization in the α zone at different temperatures for Mn 55000: (A) 145, (B) 140, (C) 135, (D) 130, (E) 125, and (F) 120°C

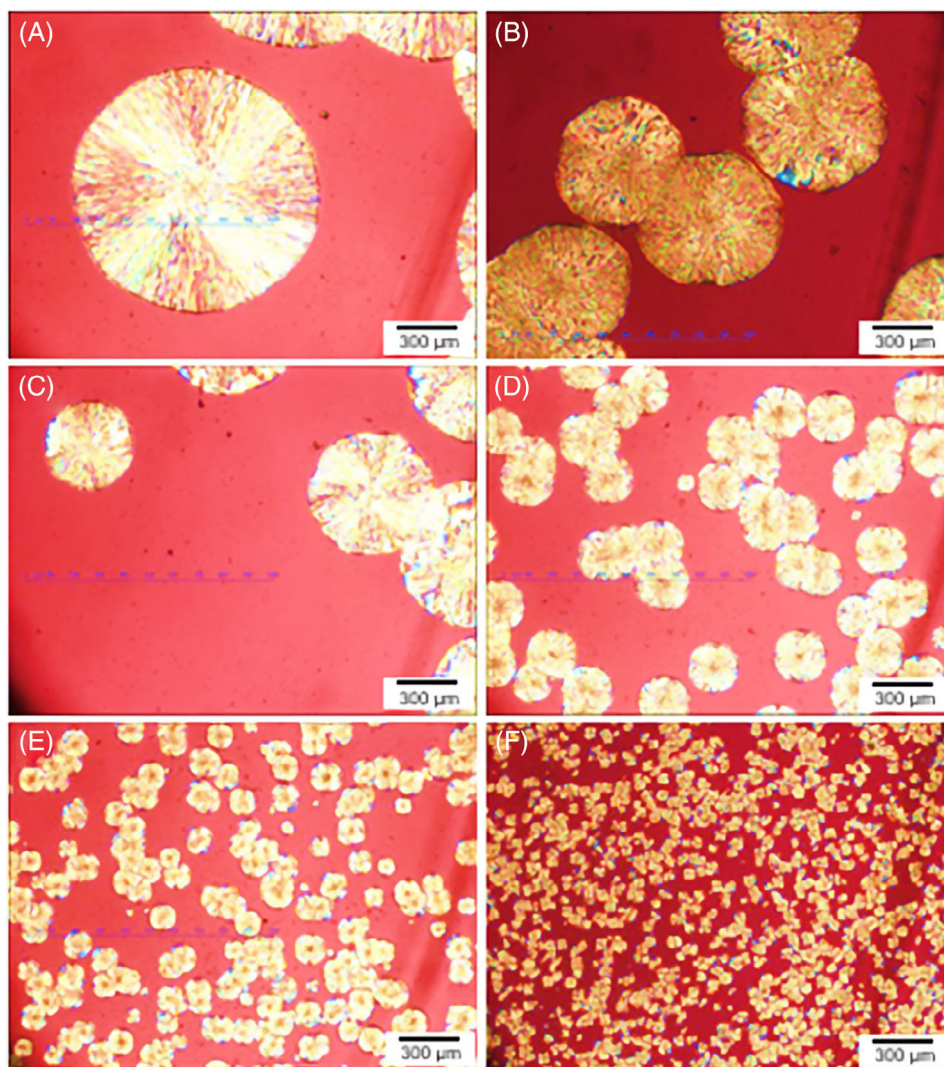
10000, respectively. Depending on the nucleation rate, size of spherulites observed in a range of 10–900 microns in diameter. For Mn 55000, the spherulites formed between 125 and 120°C were “Maltese cross” type characteristic of the lamellar structure of the polymers.^{39,44} The “Maltese cross” morphology is linked to the birefringence of the polymers and characterizes a good alignment of the crystalline lamellae with another one. From 130°C, the size of the spherulites is much larger and a strongly fibrillar structure was observed. This behavior has been observed at high temperatures of crystallizing.⁴⁵ In fact, when the size of the spherulites becomes too large, the amount of interlamellar amorphous phase increases, and the birefringence of the structure decreases, greatly attenuating the “Maltese cross” appearance. For Mn 10000, it can be considered that only the images at 145 and 135°C exhibits a morphology of the “Maltese cross” type which is relatively attenuated. Most of the structures showed a fibrillar appearance. As mentioned, it can be said that low molecular weight spherulites contain more interlamellar amorphous phases. However, the quality of the spherulites and in particular their geometry appears to be greatly altered. Indeed, one obtains

spherulites that are not completely circular anymore; moreover, it is interesting to note that at the beginning of their growth, these spherulites present a perfectly hexagonal geometry as illustrated in Figure 11 at 145°C.

In the mixed zone, due to the high nucleation, observation of the spherulites morphology is more difficult. In addition, given the sample thickness (2 μm) and the magnification used, because the nucleus formed is present on several planes it becomes difficult to obtain clear pictures of the entire sample. In both cases, the presence of more or less circular entities, in the form of a “Maltese cross” can be observed. These axialities can be attributed to nascent spherulites, which did not have enough time to form.

In the α' zone, observation is also difficult due to the abundance of the nucleus. However, the morphology of the crystals shows the presence of axialites or structures in the “Maltese cross” strongly contrasted. When the contrast between the branches becomes significantly high, it indicates that the orientation of the lamellae is much more disordered. This aspect is consistent with the hypothesis that the α' form is a disordered form.

FIGURE 12 Crystallization in the α zone at different temperatures for Mn 10000: (A) 145, (B) 140, (C) 135, (D) 130, (E) 125, and (F) 120°C



4 | CONCLUSION

The crystallization of the polymorphic PLA NW30 under the isothermal and non-isothermal conditions has been characterized. Different analytical methods have been used to quantify the contribution of these two forms of spherulites. The tests have been performed on samples with different molecular weights in order to study the role of this parameter during crystallization and its effect on the formation of crystalline morphology of the polymer. The results of DSC tests revealed that the crystalline phase of PLA NW30 could appear in two different spherulite forms, α and α' and the formation of these two forms show different kinetics and enthalpies. It was also shown that the crystallization of PLA NW30 is very slow and it can be influenced by the cooling rate especially when this later is high. This is why it does not generally fully crystallize during cooling. The quantitative study has permitted to determine the rate of crystallization. The spherulites' growth and the nucleation rate of the α -form, then were estimated.

Direct observations by optical microscope show that the nucleation and the morphology of these two forms spherulites, α and α' were influenced by the molecular weight. For the Mn 55000 and Mn

19000 samples, the nucleation rates are almost similar in comparison with the Mn 10000 and Mn 7500 samples which have lower nucleation density. For sample Mn 55000, the spherulites formed between 125 and 120°C were “Maltese cross” type with lamellar structure.

DATA AVAILABILITY STATEMENT

The data that support the findings of this study are available from the corresponding author upon reasonable request.

ORCID

Nader Zirak  <https://orcid.org/0000-0001-8551-6943>

Mohammadali Shirinbayan  <https://orcid.org/0000-0002-2757-8529>

Sedigheh Farzaneh  <https://orcid.org/0000-0001-9154-4414>

Abbas Tcharkhtchi  <https://orcid.org/0000-0003-2026-5084>

REFERENCES

1. Groot WJ, Borén T. Life cycle assessment of the manufacture of lactide and PLA biopolymers from sugarcane in Thailand. *Int J Life Cycle Assess.* 2010;15:970-984.

2. Jacobsen S, Fritz HG, Degée P, Dubois PH, Jérôme R. Polylactide (PLA)—a new way of production. *Polym Eng Sci.* 1999;39:1311-1319.
3. Farah S, Anderson DG, Langer R. Physical and mechanical properties of PLA, and their functions in widespread applications—a comprehensive review. *Adv Drug Deliv Rev.* 2016;107:367-392.
4. López-Rodríguez N, López-Arraiza A, Meaurio E, Sarasua JR. Crystallization, morphology, and mechanical behavior of polylactide/poly (ϵ -caprolactone) blends. *Polym Eng Sci.* 2006;46:1299-1308.
5. Ahmed J, Varshney SK. Polylactides—chemistry, properties and green packaging technology: a review. *Int J Food Prop.* 2011;14:37-58.
6. Saeidlou S, Huneault MA, Li H, Park CB. Poly (lactic acid) crystallization. *Prog Polym Sci.* 2012;37:1657-1677.
7. Harris AM, Lee EC. Improving mechanical performance of injection molded PLA by controlling crystallinity. *J Appl Polym Sci.* 2008;107:2246-2255.
8. Li S, McCarthy S. Influence of crystallinity and stereochemistry on the enzymatic degradation of poly(lactide)s. *Macromolecules.* 1999;32:4454-4456.
9. Wasanasuk K, Tashiro K. Crystal structure and disorder in poly (L-lactic acid) δ form (α' form) and the phase transition mechanism to the ordered α form. *Polymer.* 2011;52:6097-6109.
10. Zhang J, Tashiro K, Tsuji H, Domb AJ. Disorder-to-order phase transition and multiple melting behavior of poly (L-lactide) investigated by simultaneous measurements of WAXD and DSC. *Macromolecules.* 2008;41:1352-1357.
11. Kolmogorov AN. On the statistics of the crystallization process in metals. *Bull Akad Sci.* 1937;1:355-359.
12. Avrami M. Kinetics of phase change. I General theory. *J Chem Phys.* 1939;7:1103-1112.
13. Evans UR. The laws of expanding circles and spheres in relation to the lateral growth of surface films and the grain-size of metals. *Trans Faraday Soc.* 1945;41:365-374.
14. Foglia F, De Meo A, Iozzino V, Volpe V, Pantani R. Isothermal crystallization of PLA: nucleation density and growth rates of α and α' phases. *Can J Chem Eng.* 2020;98:1998-2007.
15. Dai X, Zhang Z, Chen C, Li M, Tan Y, Mai K. Non-isothermal crystallization kinetics of montmorillonite filled β -isotactic polypropylene nanocomposites. *J Therm Anal Calorim.* 2015;121:829-838.
16. Friedman HL. Kinetics of thermal degradation of char-forming plastics from thermogravimetry. Application to a phenolic plastic. *J Polym Sci Part C Polym.* 1964;6:183-195.
17. Vyazovkin S. Is the Kissinger equation applicable to the processes that occur on cooling? *Macromol Rapid Commun.* 2002;23:771-775.
18. Wu L, Hou H. Isothermal cold crystallization and melting behaviors of poly(L-lactic acids) prepared by melt polycondensation. *J Appl Polym Sci.* 2010;115:702-708.
19. Pantani R, De Santis F, Sorrentino A, De Maio F, Titomanlio G. Crystallization kinetics of virgin and processed poly(lactic acid). *Polym Degrad Stab.* 2010;95:1148-1159.
20. Tsuji H, Tezuka Y, Saha SK, Suzuki M, Itsuno S. Spherulite growth of L-lactide copolymers: effects of tacticity and comonomers. *Polymer.* 2005;46:4917-4927.
21. Pan P, Kai W, Zhu B, Dong T, Inoue Y. Polymorphous crystallization and multiple melting behavior of poly(L-lactide): molecular weight dependence. *Macromolecules.* 2007;40:6898-6905.
22. Zhou L, Ke K, Yang M-B, Yang W. Recent progress on chemical modification of cellulose for high mechanical-performance poly(lactic acid)/cellulose composite: a review. *Compos Commun.* 2021;23:100548.
23. Standau T, Zhao C, Murillo Castellón S, Bonten C, Altstädt V. Chemical modification and foam processing of polylactide (PLA). *Polymers.* 2019;11:306.
24. Yang B, Wang D, Chen F, et al. Melting and crystallization behaviors of poly (lactic acid) modified with graphene acting as a nucleating agent. *J Macromol Sci Part B.* 2019;58:290-304.
25. Feng Y, Ma P, Xu P, et al. The crystallization behavior of poly (lactic acid) with different types of nucleating agents. *Int J Biol Macromol.* 2018;106:955-962.
26. Pan P, Yang J, Shan G, Bao Y, Weng Z, Inoue Y. Nucleation effects of nucleobases on the crystallization kinetics of poly(L-lactide). *Macromol Mater Eng.* 2012;297:670-679.
27. He Y, Fan Z, Hu Y, Wu T, Wei J, Li S. DSC analysis of isothermal melt-crystallization, glass transition and melting behavior of poly(L-lactide) with different molecular weights. *Eur Polym J.* 2007;43:4431-4439.
28. Li M, Hu D, Wang Y, Shen C. Nonisothermal crystallization kinetics of poly(lactic acid) formulations comprising talc with poly (ethylene glycol). *Polym Eng Sci.* 2010;50:2298-2305.
29. Di Lorenzo ML, Rubino P, Luijckx R, Hérou M. Influence of chain structure on crystal polymorphism of poly(lactic acid). Part 1: Effect of optical purity of the monomer. *Colloid Polym Sci.* 2014;292:399-409.
30. Su Z, Guo W, Liu Y, Li Q, Wu C. Non-isothermal crystallization kinetics of poly(lactic acid)/modified carbon black composite. *Polym Bull.* 2009;62:629-642.
31. Tsuji H, Takai H, Fukuda N, Takikawa H. Non-isothermal crystallization behavior of poly(L-lactic acid) in the presence of various additives. *Macromol Mater Eng.* 2006;291:325-335.
32. Rathi S, Kalish JP, Coughlin EB, Hsu SL. Utilization of oligo(lactic acid) for studies of chain conformation and chain packing in poly(lactic acid). *Macromolecules.* 2011;44:3410-3415.
33. Kalish JP, Aou K, Yang X, Hsu SL. Spectroscopic and thermal analyses of α' and α crystalline forms of poly(L-lactic acid). *Polymer.* 2011;52:814-821.
34. Cocca M, Di Lorenzo ML, Malinconico M, Frezza V. Influence of crystal polymorphism on mechanical and barrier properties of poly(L-lactic acid). *Eur Polym J.* 2011;47:1073-1080.
35. Courgneau C, Domenek S, Lebossé R, Guinault A, Avérous L, Ducruet V. Effect of crystallization on barrier properties of formulated polylactide. *Polym Int.* 2012;61:180-189.
36. Abbasnezhad N, Zirak N, Shirinbayan M, et al. Controlled release from polyurethane films: drug release mechanisms. *J Appl Polym Sci.* 2021; 138:50083.
37. Chen X, Hou G, Chen Y, Yang K, Dong Y, Zhou H. Effect of molecular weight on crystallization, melting behavior and morphology of poly(trimethylene terephthalate). *Polym Test.* 2007;26:144-153.
38. Wang X, Yain D, Tian G, Li X. Effect of molecular weight on crystallization and melting of poly (trimethylene terephthalate). 1: Isothermal and dynamic crystallization. *Polym Eng Sci.* 2001;41:1655-1664.
39. Núñez E, García P, Gedde UW. Crystallisation behaviour and crystal rearrangement of poly(ethylene oxybenzoate). *Mater Sci Eng.* 2005; 413:435-441.
40. Di Lorenzo ML. Crystallization behavior of poly (L-lactic acid). *Eur Polym J.* 2005;41:569-575.
41. Yasuniwa M, Tsubakihara S, Iura K, Ono Y, Dan Y, Takahashi K. Crystallization behavior of poly(L-lactic acid). *Polymer.* 2006;47:7554-7563.
42. Bourbigot S, Garnier L, Revel B, Duquesne S. Characterization of the morphology of iPP/sPP blends with various compositions. *Express Polym Lett.* 2013;7:224-237.
43. Müller AJ, Avila M, Saenz G, Salazar J. Crystallization of PLA-based materials. *Poly(lactic acid) Sci Technol: Process Prop Addit Appl.* 2015; 2015:66-98.
44. Hoffman JD, Miller RL. Kinetic of crystallization from the melt and chain folding in polyethylene fractions revisited: theory and experiment. *Polymer.* 1997;38:3151-3212.
45. Lee WD, Yoo ES, Im SS. Crystallization behavior and morphology of poly (ethylene 2, 6-naphthalate). *Polymer.* 2003;44:6617-6625.

How to cite this article: Zirak N, Shirinbayan M, Farzaneh S, Tcharkhtchi A. Effect of molecular weight on crystallization behavior of poly (lactic acid) under isotherm and non-isotherm conditions. *Polym Adv Technol.* 2022;1-10. doi:10.1002/pat.5603